INSIGHTS INTO THE JCO CRITICALITY INCIDENT USING THE COUPLED RADIATION/MULTIPHASE CODE FETCH

Christopher C. Pain, Cassiano R. E. de Oliveira,
Matthew D. Eaton and Antony J. H. Goddard

Computational Physics and Geophysics Group
Department of Earth Science and Engineering,
Imperial College of Science, Technology and Medicine,
Prince Consort Rd, London SW7 2BP, UK

ABSTRACT

In this work we use the coupled neutronics/multi-phase code FETCH to illustrate some of the physics behind the JCO criticality incident. More specifically we focus on the physics and the associated fission oscillations of the short term (seconds) criticality behaviour of the incident. This physics involves free surface waves and radiolytic gas bubble generation mechanisms.

1. INTRODUCTION

The FETCH transient code [1] has been developed, as a generic reference method for modelling fissile solution criticality. The main features incorporated into the model are the ability to model complex geometries and spatial variations in properties and, as far as possible to model the physical processes in sufficient detail. While there existed criticality assessment codes [2], based on conservative, generic principles, the general aims for the resulting model were:

- to be a future resource for deeper understanding of complex criticality issues, for example complex reflected or interacting systems; sloshing in shallow vessels and stratified aqueous/organic mixtures - to be able to explore (that is to extrapolate to) scenarios somewhat beyond the range of experiment. An example would be the transient criticality of dilute plutonium matrices that might be formed if plutonium were translocated from a waste repository.

In this study we used data from the incident at the JCO Company on 30-31 September 1999 to: (i), gain an understanding of the mechanism of criticality to improve the future safety designs of the fuel cycle facilities and, (ii), to understand the mechanisms of this accident.

2. THE FETCH MODEL

The FETCH code comprises three modules; two transient, three-dimensional finite element modules - the neutron transport code EVENT [3] and the CFD/multiphase code FLUIDITY [4] coupled through an interface module. The transient criticality has been validated in [1,5,6,7]. In

the transient criticality validation exercises [1,5,6,7] CRAC, SILENE and TRACY experiments (see [8,9]) have been modelled. FETCH has also been used to model situations before where no experimental information is available such as for transients in dilute Pu solutions with positive temperature coefficients, see [1]. In the JCO incident some information is available from the dosimetry of the two workers irradiated [10] and from gamma detectors [11]. The dosimetry can provide an indication of the yield in the initial parts of the transient and the gamma detectors provide an indication of the oscillations that occurred in the fission-power.

At each time step the interface module of FETCH organises the feedback from FLUIDITY of spatial temperatures, densities and delayed neutron precursor distributions, into the EVENT neutronics module. It also, in the light of these fields, updates the spatial distribution of multi-group neutron cross sections for EVENT. For a given element in the finite element mesh a cross section is obtained by interpolation in temperature and voidage (due to gases) in a cross section set. This set has been condensed taking into account resonance self-shielding and thermal temperature effects, into six groups using the WIMS code [12] and a representative geometry. The neutronics module generates spatial distributions of fission rate (energy deposition) and the resulting contribution to the field of dissolved radiolytic gas concentration, for FLUIDITY. Integrated into the multi-phase method is a model for free surface motion, so that buoyancy and bubble bursting free surface motion may be modelling together with its interaction with system criticality.

3. JCO INCIDENT

Our analysis of the JCO incident, with the aid of the FETCH code, has used the best available information in performing both step reactivity transients and 'continuous filling' transients. There must be uncertainty as to how long the operators continued filling the precipitation tank after the first criticality pulse. Figure 1a shows the finite element axi-symmetric representation of the precipitation tank and its water jacket.

The Uranyl nitrate solution in question contained 370 g/ℓ of Uranium with 10$\%$ Enrichment and the molarity of nitric acid was less than 0.5 (0.5 was assumed in the modelling presented). In total, 7 batches of solution was prepared, with each batch containing about 6.5 litres of solution. Total dissolved uranium was 16.7771kg, but 182.7g was found outside of the tank, thus about 16.6kg of U was considered to be poured into the tank. In pouring, a batch was divided into 2 beakers (max. volume of beaker is 5 litre). The estimated pouring time is about 5 to 16 second for 3 litres.

After the completion of the filling activity, there would be a slower transition to 'steady' fission power, with this transition being marked by slow power oscillations on a time-scale of the heat transfer from the precipitation tank (not shown).

4. TRANSIENT SIMULATIONS

Here we describe some of the transient simulations we have used to discover the physics behind the Tokaimura and other criticality incidents.

4.1. PROBLEM DESCRIPTION

The finite element mesh used in this investigation is shown in figure 1(a). Here it is seen the internal cavity of the precipitation tank in which the fissile solution is contained. The width of this cavity is 25cm. This is then surrounded by a water jacket containing the cooling water - the cooling effect of the water has no influence on the cause of the transient over small time scales. The water jacket is surrounded by steel. The flow of radiation is modelled throughout the entire domain of the precipitation tank and surrounding water jacket. The multiphase fluid flow equations are solved only in the precipitation tank. These consist of a set of conservation equations for the liquid and another set for the gas phases.

For simulation purposes the precipitation tank is divided vertically into 3 regions, see figure 1a. The lower region contains the solution when the free surface is flat and there are no bubbles in the solution. However, we initialise all the transients here with a uniformly mixed solution containing bubbles of a volume fraction such that the solution plus bubbles occupy the lower two regions shown in figure 1(a). The lower two regions extend to a height of 30 cm above the base of the precipitation tank. So as the bubbles rise out of the solution the reactivity increases. This simple method of introducing the ramp reactivity insertion, which depends on the bubble size (1mm diameter radiolytic gas bubbles assumed here), although unphysical, is motivated by the indications (see [13] and [14]) that the magnitude of the ramp reactivity insertion does not have a big effect on the initial fission spike. Also this method of introducing a ramp has the desirable effect that it does not greatly perturb the free surface. We do not want to excite free surface waves at the beginning of the transient as this could produce a large yield in the initial fission spike.

In the simulations conducted here two solution quantities were used. One which had an excess reactivity of $3\$$ and the other had an excess reactivity of $5\$$ when there are no bubbles in the solution and the free surface is flat and the temperature is at 20^{o}C. 20^{o}C is the initial temperature assumed in these simulations. All simulations were conducted in axi-symmetric coordinates.

4.2. TRANSIENT RESULTS

As the bubbles rise out of the solution from the bubbly solution (initial condition) eventually the system goes supercritical. This then results in a rapid rise in the neutron population which eventually heats up the solution and deposits radiolytic gases into it. Both the increase in temperature (Doppler broadening) and production of bubbles (increase in neutron leakage) will have a negative reactivity effect and will reduce the fission rate. Thus there will be an initial fission spike. The mass of bubbles and the liquid temperature field just after this fission spike is seen in figures 1(b) and 1(c) respectively. Some further 2.5 seconds into the transient various fields are drawn in figures 2. At this instance in time (5 seconds into the transient) the free surface is oscillating and due to bubble induced buoyancy forces overturning of the liquid has occurred. The bubble and temperature distributions can be seen to be mixing well into the liquid, see figures 2(a),(b). At this same time level the shortest lived delayed neutron precursor concentration which has a half life of 0.2 seconds and reflects the instantaneous power distribution is drawn in figure 2(c). This shows that most of the fission-heat energy and therefore radiolytic-gas bubbles are

deposited in the central region of the domain.

4.2.1 Bubble Stratification

At some 9.5 seconds into the transient the radiolytic gas bubbles are preventing the system from becoming supercritical and thus in some sense the bubble generation is such that the system has a K_{eff} of about unity. Thus at this stage in the transient bubbles act in a similar way to increases in solution temperature in transients with lower power outputs, see [6]. The result is that the liquid volume fraction is stratified, see figure 3(a) in a similar manner to which density (temperature) becomes stratified in low powered transients. At this same time level it can be seen that the temperature field has become well mixed and more uniform, see figure 3(b). The corresponding power distribution is shown in figure 3(c).

4.2.2 Free Surface and Bubble Production Oscillations

The fission rate versus time for the simulation conducted with a relatively large neutron source of 10^6 neutrons cm^{-3} in each of the six neutron energy groups is seen in figure 4(a) along with the corresponding maximum liquid temperature versus time graph 4(b). Notice that the fission rate becomes quite oscillatory in figure 4(a). This is due to free surface waves which are caused by the mass of radiolytic gas bubbles rising to, and perturbing, the free surface and are also excited by further production of gases as the solution sloshes to the centre of the tank. The period of this oscillation is about 0.5 seconds (wave speed about 1 m/s) which matches the speed $c = \sqrt{gH} \approx 1.4$ m/s (g is gravity and H is an approximate depth of solution) of propagation of free surface waves in the simplified shallow water equations.

For a simulation conducted with a reduced neutron source of 10^3 neutrons cm^{-3} the resulting yield in the first fission spike along with the temperature is greater, compare figures 4(a) and 4(b) with figures 5(a) and 5(b). This occurs because the neutron population rises to increase the solution temperature sooner when the neutron source is larger. Thus at this point in the transient the excess reactivity caused by the ramp is smaller.

A simulation was also conduced with the solution having an excess reactivity of $5\$$ with no bubbles, a flat free surface and ambient conditions. However, the yield for this case is very similar to the previous cases because it is the ramp magnitude and neutron source that are important, see figure 6.

4.2.3 Interpretation of Transient results

When these simulations were performed for a longer period of time there is a second broad fission spike associated with the gradual removal of bubbles our of the system and interaction with reactivity with delayed neutrons, see [15]. Thus one should expect further fission oscillations associated on a time scale of the rise of radiolytic gas bubbles out of the system. In addition, free surface waves, which propagate with a well defined velocity and result in a characteristic signature in the fission rate versus time graphs, would be expected, see simulations of the CRAC experiments [16].

In the JCO incident the workers would have carried on pouring some time after the initial fission spike. This would have resulted in an increase in the potential reactivity of the system. This would have increased the likelihood of further fission oscillations of the types reported here.

5. CONCLUSIONS

A fundamentally-based, transient criticality model, incorporated into the FETCH code, has been described and applied to the JCO criticality incident. We show that due to some fundamental modelling features FETCH may be applied not only to scenarios somewhat outside the range of experiment, but may further be applied to design studies aimed at producing safer facilities.

REFERENCES

1. C.C. Pain, C.R.E. de Oliveira, A.J.H. Goddard and A.P. Umpleby, "Criticality behaviour of dilute plutonium solutions", *Nucl. Sci. Tech.*, **135**, pp. 194-215 (2001).
2. J.J. Duderstadt, and L.J. Hamilton, *Nuclear reactor analysis.* Wiley, New York (1976).
3. C.R.E. de Oliveira, "An arbitrary geometry finite element method for multigroup neutron transport with anisotropic scattering", *Prog. Nucl. Energy.*, **18**, pp 227-236 (1986).
4. S. Mansoorzadeh, C.C. Pain, C.R.E. de Oliveira and A.J.H. Goddard, "Finite element simulations of incompressible flow past a heated/cooled sphere", *Int. J. Num. Methods. Fluids.*, **28**, pp. 903-915 (1998).
5. C.C. Pain, C.R.E. de Oliveira, A.J.H. Goddard and A.P. Umpleby, "Transient criticality in fissile solutions - compressibility effects", *Nucl. Sci. Eng.*, **138**, pp. 78-95 (2001).
6. C.C. Pain, C.R.E. de Oliveira and A.J.H. Goddard, "Non-linear space-dependent kinetics for criticality assessment of fissile solutions", *Prog. Nucl. Energy*, **39**, pp. 53-114 (2001).
7. C.C. Pain, A.J.H. Goddard and C.R.E. de Oliveira, "The finite element transient criticality code FETCH - verification and validation", *Proceedings of the second NUCEF international symposium on nuclear fuel cycle, Hitachinaka, Ibaraki, Japan*, pp. 139 (1998).
8. "Fissile solution criticality accidents - review of pressure wave measurements experiments in the SILENE reactor", *Institut de protection et de surete nucleaire, technical note SRSC no. 87.96.*, (1987).
9. K. Ogawa, K. Nakajima, H. Yanagisawa, H. Sono, E. Aizawa, T. Morita, S. Sugawara, K. Sakuraba and A. Ohno, "Measurement of power profile during nuclear excursions Initiated by Various Reactivity Additions using Tracy", *Proceedings of the sixth international conference on nuclear criticality safety, Versailles, France.*, (1999).
10. M. Akashi, "Exposure to neutron irradiation in the criticality accident in Tokaimura", *Division of Radiological Sciences Report*, (2000).

11. "The Report of the Uranium Processing Plant Criticality Accident Investigation Committee", *Committee of the nuclear safety commission*, Dec 1999.

12. WIMS8A: User Guide for Version 8, *AEA Technology Report ANSWERS/WIMS(99)9* (1999).

13. C.C. Pain, C.R.E. de Oliveira, A.J.H. Goddard, M.D. Eaton, S. Gundry and A.P. Umpleby, "Transient analysis and dosimetry of the Tokaimura criticality accident", (in preparation).

14. K. Nakajima, et al. *Proceedings of the international seminar on nuclear criticality safety, Tokyo Symposium, Tokaimura, Japan*, Oct 31 - Nov 2, (2001).

15. C.C. Pain, Y. Yamane, A.J.H. Goddard and C.R.E. de Oliveira, "Status of the FETCH transient criticality code and application to TRACY data and dosimetry applications", *Proceedings of the 3nd NUCEF International Symposium, Tokaimura, Japan*, Oct 31 - Nov 2, (2001).

16. C.C. Pain, C.R.E. de Oliveira and A.J.H. Goddard, "Modelling the criticality consequences of free-surface motion in fissile liquids", *Proceedings of the 2nd NUCEF international symposium, Hitachinaka, Ibaraki, Japan*, Nov 16-17, (1998).

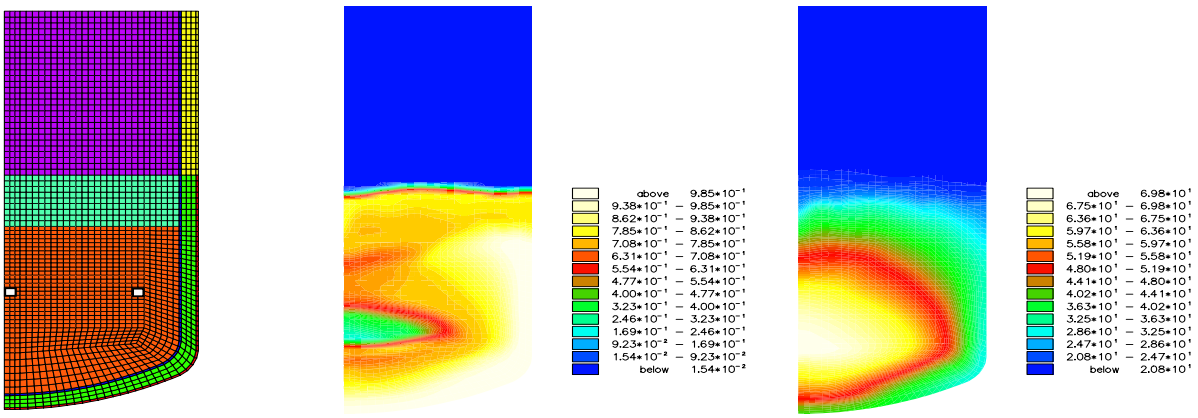

(a) Finite element mesh (b) liquid volume fraction (c) liquid temperature

Figure 1: Diagram showing the mesh used in the transients and a mass of radiolytic gas bubbles deposited just after the first fission spike rising to the free surface (a) and (b) the corresponding temperature distribution. At 2.5 seconds into the simulations and low neutron source simulation.

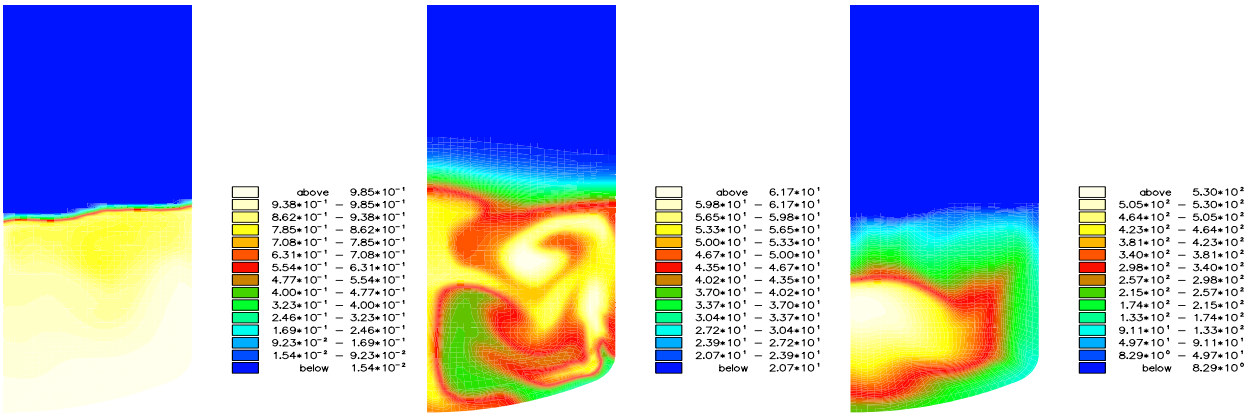

(a) liquid volume fraction (b) liquid temperature (c) delayed concentration

Figure 2: Diagram showing the liquid volume fraction, temperature and shortest delayed group concentration at 5.0 seconds into the transient with a small neutron source.

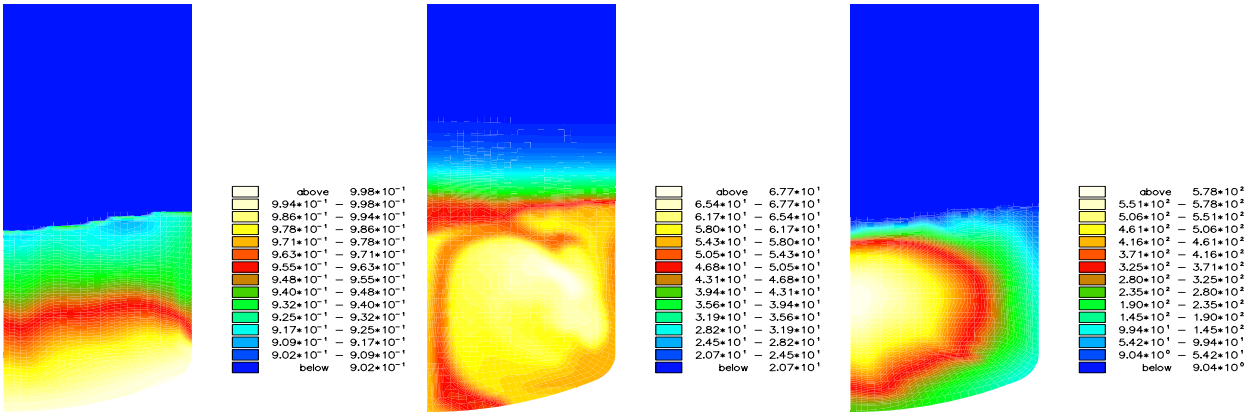

(a) liquid volume fraction (b) liquid temperature (c) delayed concentration

Figure 3: The stratified liquid volume fraction, temperature and shortest lived delayed neutron precursor concentration (power distribution) at 9.5 seconds into the simulation with a large neutron source.

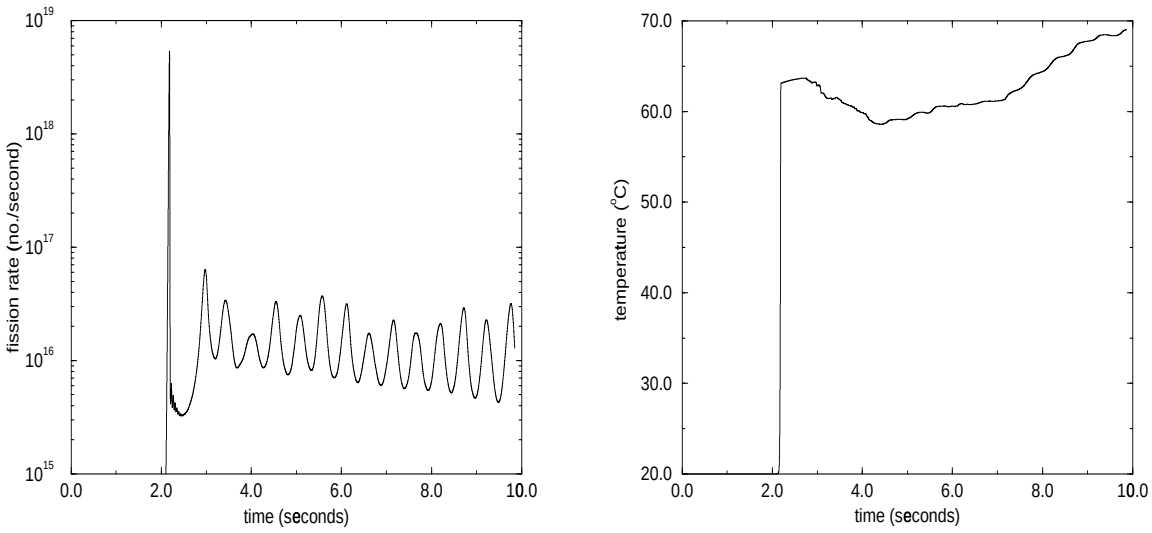

(a) fission rate (b) maximum liquid temperature

Figure 4: Fission rate and maximum liquid temperature versus time for the simulation conducted with a large neutron source.

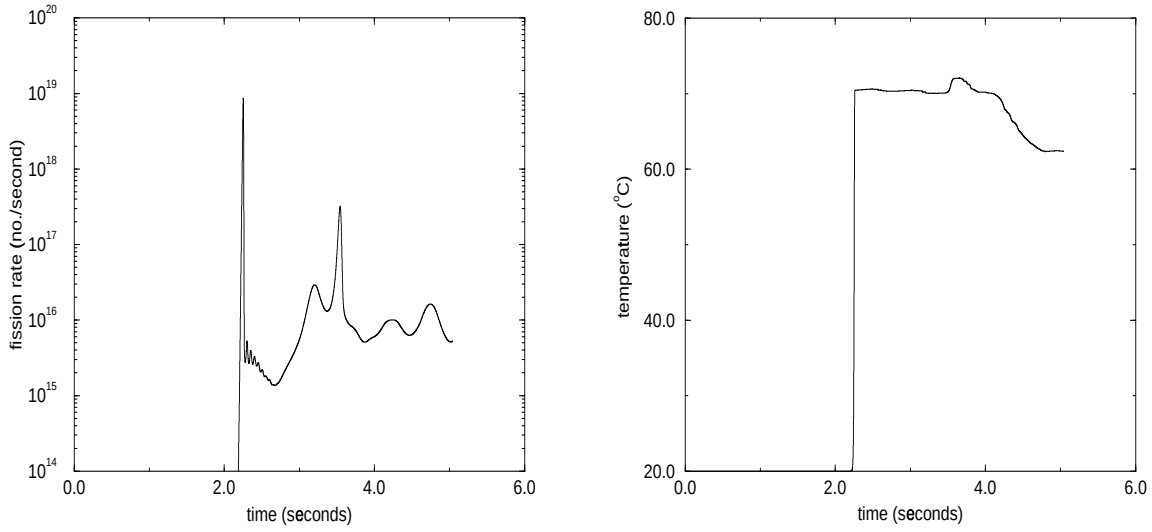

(a) fission rate (b) maximum liquid temperature

Figure 5: Fission rate and maximum liquid temperature versus time for the simulation conducted with a small neutron source.

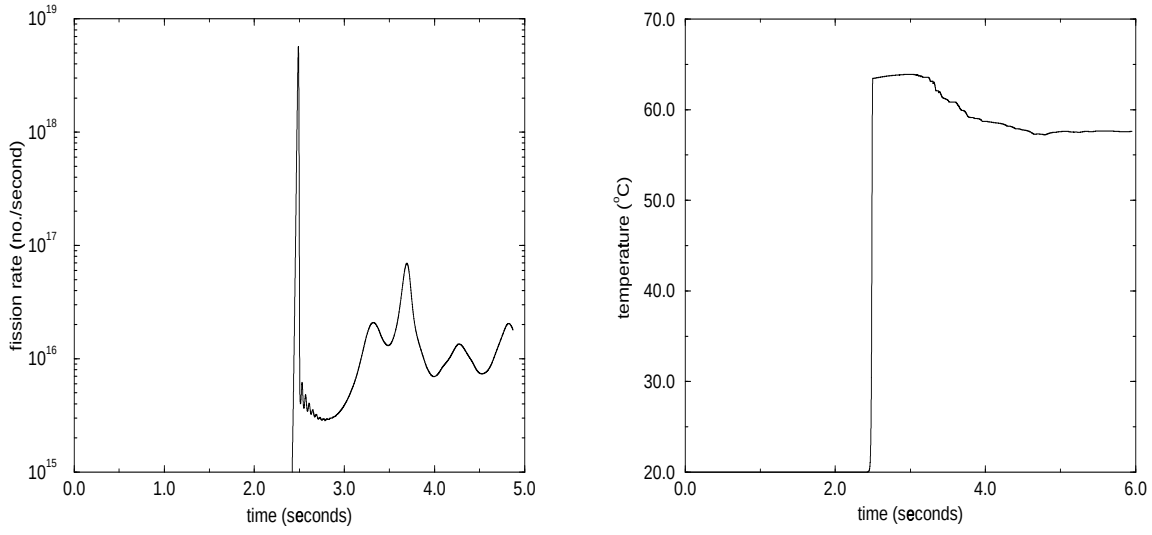

(a) fission rate (b) maximum liquid temperature

Figure 6: Fission rate and maximum liquid temperature versus time for the simulation conducted with a large neutron source and a large potential reactivity